Electrocatalysis on Gold Clusters

DOI: 10.1002/anie.200905614

Aqueous CTAB-Assisted Electrodeposition of Gold Atomic Clusters and Their Oxygen Reduction Electrocatalytic Activity in Acid Solutions**

*Chinnaiah Jeyabharathi, Shanmugam Senthil Kumar, Gobichettipalayam Venkataramani Manohar Kiruthika, and Kanala Lakshmi Narasimha Phani**

Dedicated to Dr. Gollakota Prabhakara Rao and in memory of Sarukkai Krishnamachari Rangarajan

In a modification of Reetz's electrochemical production of metal nanoparticles from surfactant solutions,[1,2] Yu et al.[3] observed the generation of gold nanorods exhibiting both transverse and longitudinal surface plasmon resonance (SPR). This method uses a gold metal sheet as anode and platinum as cathode in a mixed surfactant solution of cetyltrimethylammonium bromide (CTAB) and a rod-shape-inducing co-surfactant. This observation triggered a flurry of activity in nanocatalysis and plasmonic sensors. However, the aspects of particle growth and evolution of nanostructures remain unexplored. Interesting questions to ask are: 1) is the growth of different Au nanostructures preceded by the formation of stable gold clusters of a few atoms (zone between molecular and nanoscale structures); and 2) how (electro-) catalytic are these clusters? Nanosized gold particles have been examined extensively as active catalysts for CO oxidation[4–7] and the oxygen reduction reaction (ORR).[8,9] However, most of the earlier studies were concerned with Au nanoparticles that are larger than 2 nm in diameter. The high catalytic activity of clusters of about ten gold atoms (ca. 0.5 nm in diameter) towards CO oxidation[10] suggests that subnanometer-sized clusters represent a unique class of catalysts.

In situ spectroscopic investigations of gold electrooxidation/re-reduction in CTAB-containing solutions in the present work have provided some of the most intriguing glimpses of the initial stages of nanoparticle production. We observed molecule-like absorption bands typical of gold clusters of a few atoms, examined by using a UV/Vis optical-fiber probe placed near the gold working electrode. The total absence of the SPR bands suggested an interesting possibility that the initial products are not nanoparticles but clusters of a few atoms.[11]

Herein, we show that the clusters deposited on gold and glassy carbon exhibit 1) molecule-like voltammetric features typical of the redox chemical character of smaller core clusters;[12] and 2) a smooth transition from an electrocatalytic four-electron to a bulk-type two-electron reduction pathway in the catalytic behavior towards a structure-sensitive reaction such as oxygen reduction, depending on the CTAB concentration used during the electrochemical synthesis of gold atomic clusters (AuACs).

When a clean gold-disk electrode is cycled in a solution containing CTAB (less than the critical micelle concentration (cmc), 0.1 mM, or >cmc, 50 mM) in a potential region from 0.48 to 1.88 V versus the standard hydrogen electrode (SHE) for 50 cycles at a scan rate of $100\,mV\,s^{-1}$, AuACs are generated on the electrode surface. An orange-yellow film was seen on the gold electrode when [CTAB] = 50 mM (see the Supporting Information), whereas no visually distinguishable film was obtained when [CTAB] = 0.1 mM. Simultaneously, the course of potential cycling was monitored by using an in situ UV/Vis probe, which exhibited the signature features of molecule-like subnanometer gold clusters.[13–15]

The optical spectrum (Figure 1) is more structured within each of the bands and gives major and minor bands at 393,

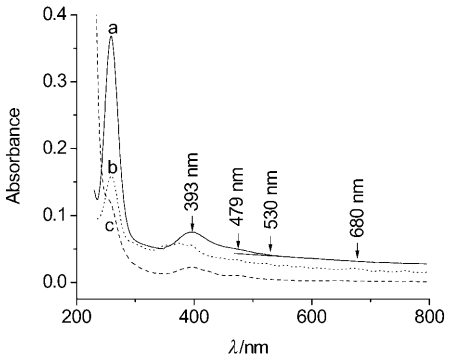

Figure 1. UV/Vis spectra of AuACs a) in CTAB/H_2O (——), b) in Bu_4NClO_4/CH_2Cl_2 (••••), and c) deposited on glassy carbon and dissolved in Bu_4NClO_4/CH_2Cl_2 (-----).

[*] C. Jeyabharathi, Dr. S. Senthil Kumar, Dr. K. L. N. Phani
Nanoscale Electrocatalysis & Sensor Research Group
Electrodics & Electrocatalysis Division
CSIR-Central Electrochemical Research Institute
Karaikudi 630 006 (India)
Fax: (+91) 4565-227-779
E-mail: kanalaphani@gmail.com

Dr. G. V. M. Kiruthika
X-ray Photoelectron Spectroscopy Laboratory of CIF
CSIR-Central Electrochemical Research Institute
Karaikudi 630 006 (India)

[**] C.J. thanks CSIR for a research fellowship, K.L.N.P. acknowledges financial support from DST-India (SR/S1/PC-37/2004), and we thank Sridevi Iyer and Prajakta Pednekar, Piramal Life Sciences–Mumbai, for MALDI-TOF mass spectrometry analysis. CTAB = cetyltrimethylammonium bromide.

Supporting information for this article is available on the WWW under http://dx.doi.org/10.1002/anie.200905614.

© 2010 Wiley-VCH Verlag GmbH & Co. KGaA, Weinheim

479, and 680 nm etc. These bands may be attributed to the interband (sp←d) and intraband (sp←sp) electronic transitions. The band at 680 nm results from an intraband electronic transition and is similar to the excitonic transition observed with semiconducting quantum dots.[16] The spectral responses for the dispersions of this orange-yellow film in H_2O/CTAB and CH_2Cl_2/Bu_4NClO_4 are very similar, and show a molecule-like behavior that is entirely different from the SPR band for the spherical gold nanoparticles.[17] For particles below about 1.5 nm in size, the SPR band is totally absent and the spectrum consists of continuously increasing absorbance with decreasing wavelength.[14] For very small clusters (Au_n, $n <$ 10–20 atoms), discrete, molecule-like bands similar to those observed in Figure 1 are expected. Based on the band-gap trend observed for these clusters,[14] the present experiments suggest the generation of Au_n clusters of $n \lesssim 13$ atoms. We speculate that the structure of these clusters is such that the smallest are protected by oligomeric motifs.[18] Also, the optical spectra of gold clusters have a band edge at about 530 nm, which corresponds to a HOMO–LUMO gap of the clusters that works out to be 2.34 eV.

In differential pulse voltammetry (Figure S1 in the Supporting Information), the redox chemical character of AuACs and a large featureless central gap of 2.5 V are the result of the molecule-like electronic energy structure of small clusters arising from their subnanometer core dimensions with a rather substantial HOMO–LUMO gap.[12] This gap agrees well with that observed in the optical spectra described above.

The core-size range of clusters indicated in the above experiments was confirmed by mass spectrometry. Matrix-assisted laser desorption/ionization time-of-flight (MALDI-TOF) mass spectrometry is emerging as an authentic tool for positive identification of nanocluster core size.[15,19,20] Figure 2 displays the mass spectrum of the electrolyzed samples, directly showing the presence of AuACs of 1034 (Au_5), 1178 (Au_6), 1791 (Au_9), 2255 (Au_{11}), and 2542 Da (Au_{13}) corresponding to a cluster size range of $5 \leq n \leq 13$, Au_5 being the most abundant cluster. As we employed a mild laser along with an organic matrix (α-cyano-4-hydroxycinnamic acid), the results are free from fragmentation. Peaks arising from the protective CTAB are not seen because its interaction with Au is weak. The Au 4f core-level photoelectron spectra of the deposits on an Au-foil electrode (Figure S2 in the Supporting Information) exhibit a positive shift of $4f_{7/2}$ binding energy from that of the bulk, which suggests the presence of small clusters surrounded by CTA^+Br^-, as carbon and bromine are also detected in the spectra. These clusters could not be imaged by analytical transmission electron microscopy, as they are too small (see the Supporting Information).

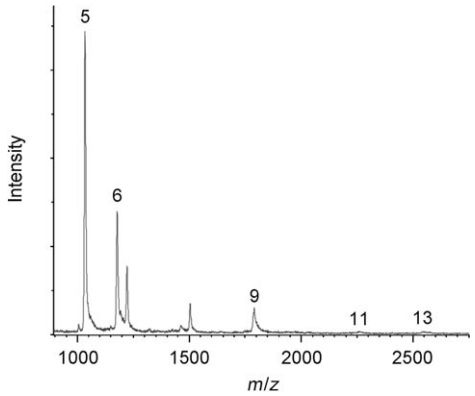

Figure 2. MALDI-TOF mass spectrum of the gold-cluster sample (index numbers indicate *n*, the number of atoms per cluster).

From the electrocatalytic point of view, bulk gold is poorly active towards the ORR in acidic media since the reduction leads not to water but only to H_2O_2 by two-electron addition. In an interesting development, Zhang et al.[21] demonstrated the replacement of a third of the platinum surface with AuACs, without affecting the electrocatalytic activity to the ORR. Other recent reports that demonstrated high ORR electrocatalytic activity through a direct four-electron addition deal with AuACs/carbon-supported particles[8,14] and Au_n ($n = 11$–140)[15] in acidic and alkaline solutions, respectively. The smallest clusters were found to yield the highest rate constant.

Figure 3 shows a comparison of the linear-sweep voltammograms for the ORR in oxygen-saturated 0.5 M H_2SO_4 solutions on 1) bulk polycrystalline gold substrate and 2) AuACs electrodeposited from 50 mM CTAB solutions. The voltammetric current density for the ORR on AuACs is twice that of the bulk gold electrode,[22] thus indicating that oxygen reduction takes place through the direct four-electron pathway. A half-wave potential of 0.025 V versus SHE of the four-electron oxygen reduction wave is approximately 0.3 V more anodic than that reported by Rodríguez-Vázquez et al.,[14] which confirms the strong electrocatalytic activity of the nanoclusters in the present work.[23] These nanoclusters reduce oxygen directly to water, as also proved by hydrodynamic voltammetry.

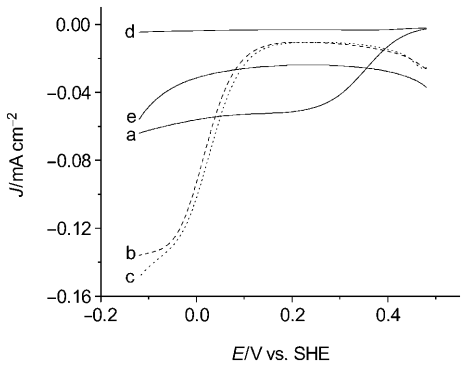

Figure 3. Linear-sweep voltammograms for the ORR in oxygen-saturated 0.5 M H_2SO_4 solution: a) on bulk polycrystalline gold substrate (——); b) on AuACs electrodeposited from 50 mM CTAB solutions (-----); and c) on Nafion-coated AuACs (•••••). d,e) Voltammograms equivalent to those in (a) and (b), respectively, in nitrogen-saturated H_2SO_4. Scan rate: 5 $mV s^{-1}$; scan direction: cathodic.

Rotating ring-disk electrode (RRDE) studies yield a value of four for the number of electrons involved in the reduction of oxygen, and a level of $\leq 1\,\%$ for the percentage

 © 2010 Wiley-VCH Verlag GmbH & Co. KGaA, Weinheim

of hydrogen peroxide generated (measured at 0.03 V vs. SHE where its generation is expected to be maximum). The current waves in the rotating disk electrode (RDE) voltammograms (Figure S5 in the Supporting Information) are very well defined, in contrast to those obtained with larger gold nanoparticles. In fact, the voltammetric patterns are akin to those observed with Pt or Pt–M bimetallic electrocatalysts.[24]

The Koutecky–Levich plots ($\omega^{-1/2}$ vs. i^{-1}) at various electrode potentials corresponding to the RDE voltammograms (Figure S5 in the Supporting Information) are perfectly linear, with slopes remaining nearly constant over a potential range of 0.22 to 0.14 V versus SHE and parallel to each other, which suggests favorable electrode kinetics of the ORR at different electrode potentials. The calculated kinetic limiting current density (J_k) and rate constant are 32 mA cm^{-2} at 0.18 V versus SHE and 6.6×10^{-2} cm s^{-1}, respectively.[25]

Some theoretical studies[26,27] have shown that a decrease in the core size of Au nanoclusters results in narrowing of the d bands shifting towards the Fermi level. The work of Metiu et al.[28] shows that roughness arising from the edges of a planar Au cluster ($n \leq 13$) acts by localizing electron density at the site, thus facilitating electronic charge transfer to the π^* orbital of O_2 which leads to bonding. The disordered nature of the CTAB micellar protecting layers on the planar Au clusters most likely exposes the catalytically active edge or defect sites. In addition, preference for O_2 binding may also depend on the cluster being neutral or negatively charged.

Gold clusters deposited from solutions of CTAB below its cmc present us with the possibility of witnessing another interesting feature of ORR electrocatalysis. The linear-sweep voltammograms presented in Figure 4 were obtained from

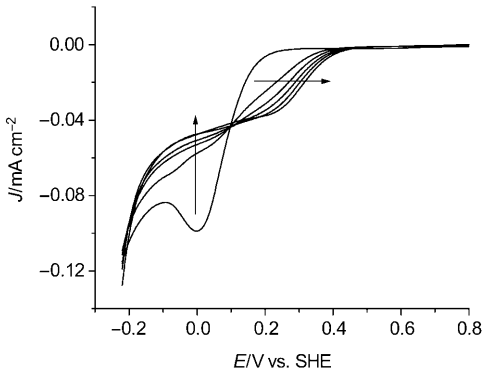

Figure 4. Successive linear-sweep voltammograms for the ORR in oxygen-saturated 0.5 M H_2SO_4 solutions on AuACs electrodeposited from 0.1 mM CTAB solutions. Scan rate: 5 mV s^{-1}; scan direction: cathodic. Arrows indicate the direction of shift of current/potential.

several consecutive runs recorded for the ORR on AuACs electrodeposited by potential cycling in 0.1 mM CTAB solutions in a potential region of 0.48 to 1.88 V versus SHE. The first scan yields a current peak at 0.01 V. In the subsequent runs using the same AuAC-covered electrode, there is a gradual decrease in current with associated: a) splitting of the current wave into two; b) shifting in the potential of the first split peak to less cathodic and of the second peak to more cathodic potentials; and c) total disappearance of the second wave because of the obvious loss of catalytic activity for H_2O_2 reduction to water. The curves corresponding to the subsequent runs cross the curve of the first run at its near mid-point. This result clearly shows that the mechanism changes to two-step two-electron reduction from what is initially a direct four-electron reduction.

This mechanism changeover also points to a possible transformation of atomic clusters to nanoparticles, an observation unprecedented in the literature of AuACs and electrochemical reactions. That the transition is caused only by the AuACs and not by the exposure of the gold substrate is proved in a control experiment with cluster-modified glassy carbon electrodes (see the Supporting Information). This dependence of the nature of the AuACs on the concentration of CTAB used in the electrosynthesis is suggestive of ineffective stabilization of AuACs at a concentration of 0.1 mM as much as when it is 50 mM, possibly because of "electrochemical sintering".

In summary, we have demonstrated that CTAB-assisted aqueous electrodeposition yields AuACs (with Au_5 being abundant) that: 1) are molecule-like; 2) electrocatalyze the reduction of oxygen to water through a direct four-electron pathway in acidic solutions; and 3) show a transition of the ORR mechanism from four-electron to two-electron reduction, which reflects the transformation of AuACs possibly to nanoparticles. From the surface science point of view, pertinent issues, such as cluster-phase formation at the electrode surfaces, the mechanism of transformation[29] of planar atomic clusters to nonplanar three-dimensional clusters or nanoparticles, and their stability under reaction conditions, need immediate attention. Work to elucidate these aspects using electrochemical-STM is underway in our laboratories.

Experimental Section

Absorbance studies of AuACs in CTAB/water and Bu_4NClO_4/CH_2Cl_2 were performed with a Cary 500 scan UV/Vis–near-IR spectrophotometer with incident light normal to the 1 cm path length quartz cuvette. For in situ observation of absorption bands during electrochemical cycling, a combination of a fiber-optic SD-2000 spectrometer with a dip-probe and DH-2000-BAL light source (Ocean Optics) was employed.

A conventional three-electrode cell was used for the electrochemical studies. The gold-disk working electrode was polished with 4/0 grade emery sheet and alumina slurry, cleaned well with Millipore water, sonicated, and then pretreated by potential cycling in sulfuric acid solutions. This clean electrode was used for electrogeneration of AuACs on its surface. Pt foil was used as counter electrode. Electrochemical measurements were performed using mercury/mercurous sulfate and quasi-silver reference electrodes. However, all the potentials reported herein are referred to the SHE, unless otherwise stated. CTAB dissolved in water played a dual role as the supporting electrolyte and surfactant stabilizer for AuACs. The cyclic/linear-sweep voltammetric experiments were carried out using a BAS-100B instrument (Bioanalytical Systems, Inc.), BIPOT module of the Autolab potentiostat/galvanostat, and RRDE setup (Pine Instruments) for hydrodynamic voltammetry. For studies on the ORR, oxygen-saturated H_2SO_4 solutions were used with an oxygen blanket maintained throughout the electrochemical measurement. All the

 © 2010 Wiley-VCH Verlag GmbH & Co. KGaA, Weinheim

solutions were prepared with Millipore water (18.2 MΩ cm) and the temperature was maintained at 25 °C.

Received: October 7, 2009
Revised: November 25, 2009
Published online: February 9, 2010

Keywords: cluster compounds · electrocatalysis · gold · oxygen electroreduction · reaction mechanisms

[1] M. T. Reetz, W. Helbig, *J. Am. Chem. Soc.* **1994**, *116*, 7401.
[2] C.-J. Huang, P.-H. Chiu, Y.-H. Wang, K.-L. Chen, J.-J. Linn, C.-F. Yang, *J. Electrochem. Soc.* **2006**, *153*, D193.
[3] Y.-Y. Yu, S.-S. Chang, C.-L. Lee, C. R. C. Wang, *J. Phys. Chem. B* **1997**, *101*, 6661.
[4] T. Hayashi, K. Tanaka, M. Haruta, *J. Catal.* **1998**, *178*, 566.
[5] M. Valden, X. Lai, D. W. Goodman, *Science* **1998**, *281*, 1647.
[6] B. E. Hayden, *Angew. Chem.* **2007**, *119*, 3600; *Angew. Chem. Int. Ed.* **2007**, *46*, 3530.
[7] F. Boccuzzi, G. Cerrato, F. Pinna, G. Strukul, *J. Phys. Chem. B* **1998**, *102*, 5733.
[8] a) I. Yagi, T. Ishida, K. Uosaki, *Electrochem. Commun.* **2004**, *6*, 773; b) T. Inasaki, S. Kobayashi, *Electrochim. Acta* **2009**, *54*, 4893.
[9] J. Hernandez, J. Solla-Gullon, E. Herrero, A. Aldaz, J. M. Feliu, *J. Phys. Chem. C* **2007**, *111*, 14078.
[10] A. Herzing, C. J. Kiely, A. F. Carley, P. Landon, G. J. Hutchings, *Science* **2008**, *321*, 1331.
[11] The reason why these molecule-like spectral features were not observed in reference [3] is that nanorod production required the use of a very high current to overcome the retarding effect of CTAB on the growth of gold seeds: M. Grzelczak, J. Pérez-Juste, P. Mulvaney, L. M. Liz-Marzán, *Chem. Soc. Rev.* **2008**, *37*, 1783.
[12] a) S. Chen, R. S. Ingram, M. J. Hostetler, J. J. Pietron, R. W. Murray, T. G. Schaaff, J. T. Khoury, M. M. Alvarez, R. L. Whetten, *Science* **1998**, *280*, 2098; b) R. Sardar, A. M. Funston, P. Mulvaney, R. W. Murray, *Langmuir* **2009**, *25*, 13840.
[13] a) Y. Y. Yang, S. W. Chen, *Nano Lett.* **2003**, *3*, 75; b) M. J. Rodríguez-Vázquez, C. Vázquez-Vázquez, J. Rivas, M. A. Lopaz-Quintela, *Eur. Phys. J. D* **2009**, *52*, 23; c) M. Zhu, C. M. Aikens, F. J. Hollander, G. C. Schatz, R. Jin, *J. Am. Chem. Soc.* **2008**, *130*, 5883; d) V. L. Jimenez, D. G. Georganopoulou, R. J. White, A. S. Harper, A. J. Mills, D. I. Lee, R. W. Murray, *Langmuir* **2004**, *20*, 6864.
[14] M. J. Rodríguez-Vázquez, M. C. Blanco, R. Lourido, C. Vázquez-Vázquez, E. Pastor, G. A. Planes, J. Rivas, M. A. Lopez-Quintela, *Langmuir* **2008**, *24*, 12690.
[15] W. Chen, S. W. Chen, *Angew. Chem.* **2009**, *121*, 4450; *Angew. Chem. Int. Ed.* **2009**, *48*, 4386.
[16] a) P. Alivisatos, *J. Phys. Chem.* **1996**, *100*, 13226; b) J. Z. Zhang, *Acc. Chem. Res.* **1997**, *30*, 423.
[17] The chances of cluster aggregation and the formation of differently shaped nanoparticles are ruled out based on the total absence of an SPR band at around 520 nm (transverse) and at higher wavelengths (longitudinal).
[18] D.-E. Jiang, W. Chen, R. L. Whetten, Z. Chen, *J. Phys. Chem. C* **2009**, *113*, 16983.
[19] A. C. Dharmaratne, T. Krick, A. Dass, *J. Am. Chem. Soc.* **2009**, *131*, 13604.
[20] Y. Zhang, S. Shuang, C. Dong, C. K. Lo, M. C. Paau, M. M. F. Choi, *Anal. Chem.* **2009**, *81*, 1676.
[21] J. Zhang, K. Sasaki, E. Sutter, R. R. Adzic, *Science* **2007**, *315*, 220.
[22] The electrochemical surface area of the gold-nanocluster film is estimated by using the oxygen adsorption method: S. Trasatti, O. A. Petrii, *J. Electroanal. Chem.* **1992**, *327*, 353. The surface area values calculated are $A = 0.045$ and $0.062\ cm^2$ for AuACs prepared using [CTAB] above and below the cmc, respectively. The surface area of the bulk gold electrode is almost same as that of the AuACs prepared using [CTAB] = 0.1 mM (i.e., below the cmc). See Figure S6 in the Supporting Information for blank voltammetry of AuACs.
[23] Deposits of AuACs are fine powders loosely bound to the AuAC-coated electrode surface, and their adhesion can be enhanced by deposition on Nafion-coated substrates (Supporting Information).
[24] W. Chen, J. M. Kim, S. H. Sun, S. W. Chen, *J. Phys. Chem. C* **2008**, *112*, 3891.
[25] A Tafel slope value of $(120 \pm 2)\ mV\,dec^{-1}$ indicates that the first electron transfer is rate-determining.
[26] J. A. van Bokhoven, J. T. Miller, *J. Phys. Chem. C* **2007**, *111*, 9245.
[27] N. S. Phala, E. van Steen, *Gold Bull.* **2007**, *40*, 150.
[28] a) G. Mills, M. S. Gordon, H. Metiu, *J. Chem. Phys.* **2003**, *118*, 4198; b) G. Mills, M. S. Gordon, H. Metiu, *Chem. Phys. Lett.* **2002**, *359*, 493.
[29] R. M. Olson, S. Varganov, M. S. Gordon, H. Metiu, S. Chretien, P. Piecuch, K. Kowalski, S. A. Kucharski, M. Musial, *J. Am. Chem. Soc.* **2005**, *127*, 1049.

 © 2010 Wiley-VCH Verlag GmbH & Co. KGaA, Weinheim

Angewandte Chemie
Eine Zeitschrift der Gesellschaft Deutscher Chemiker

Supporting Information

© Wiley-VCH 2010

69451 Weinheim, Germany

Aqueous CTAB-Assisted Electrodeposition of Gold Atomic Clusters and Their Oxygen Reduction Electrocatalytic Activity in Acid Solutions**

*Chinnaiah Jeyabharathi, Shanmugam Senthil Kumar, Gobichettipalayam Venkataramani Manohar Kiruthika, and Kanala Lakshminarasimha N. Phani**

anie_200905614_sm_miscellaneous_information.pdf

Materials: CTAB, cetyltrimethylammonium bromide (Ranchem) dissolved in water plays a dual role as a supporting electrolyte and a surfactant to stabilize gold atomic clusters (AuACs). Bu_4NClO_4, tetrabutylammonium percholate (Fluka), sulphuric acid are the other chemicals used in this study. All the solutions were prepared using Millipore water (18.2 MΩ.cm) and the temperature maintained throughout the study is 25°C.

Electrogeneration of gold atomic clusters: The potential cycling of the polycrystalline gold disk electrode in either 50 mM or 0.1mM CTAB solution for 50 consecutive runs) in a potential region from 0.48 to 1.88 V vs SHE for 50 cycles at a scan rate of 100 mVs^{-1} leads to the formation gold nanocluster film on the surface of the gold disk electrode. Then the electrode is washed using water and dried. The electrode coated with gold nanocluster film is then utilized for the electrocatalytic reaction. In the same way the gold clusters is coated on the RDE gold disk electrode for hydrodynamic voltammetric studies. Also the AuACs coated on the thin gold foil of the dimension of 0.5×0.5cm was used for x-ray photoelectron spectroscopy. For optical and DPV studies, the AuACs generated on gold disk electrode are then dispersed in Bu_4NClO_4/CH_2Cl_2 and CTAB. For TEM studies, the clusters were dispersed in acetone and placed on carbon-coated copper grid.

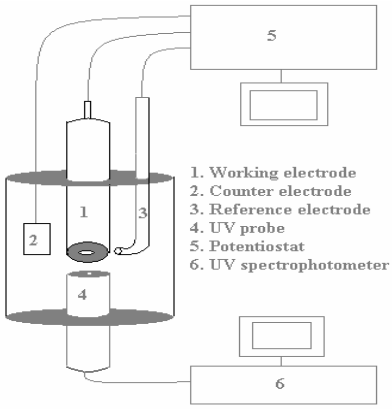

Schematic of in situ UV-Visible spectral monitoring of electrogeneration of gold clusters

Low-dimensional materials can be deposited on electrode surfaces using micellar electrodeposition that can be described by a model similar to the one presented by Naoi et al[1]. Based on this model, we suggest a possible mechanism of formation of atomic clusters that involves the following steps: (a) adsorption of micellar Au-CTAB complex on the electrode surface; (b) formation on the electrode surface of "hemi-micelles" containing gold clusters formed upon electrochemical reduction during the cathodic scan; (c) gold nuclei (atomic clusters, in the present case) surrounded by the stabilizing CTA^+ (during which growth beyond atomic clusters is stopped by CTAB micelles; (d) deposition of more mass of clusters occurs as CTAB monolayers around Au nanoclusters are known to be highly disordered[2]; deposition occurs through these defects. Development of layers of surfactant-protected clusters occurs, although limited to a particular thickness, for example, 50 potential cycles in the electrochemical treatment described above. This additional mass of clusters produced is "loosely" held to the electrode surface and can also be collected by repeated scraping off the product from the electrode. As can be explained by this model, the individual clusters are "connected" to the substrate through the defects in the CTAB monolayers. The observation of distribution in the size of the clusters suggests that the control over the size of the atomic clusters is not yet perfect. The presence of surfactant is seen from the appearance of signals for carbon and Br in the survey x-ray photoelectron spectrum (refer to Fig.S2).

The deposited layers can also be collected by repeated scraping off the product from the electrode for physical characterization.

We find, during the electrochemical cycling in region from 0.48 to 1.88 V vs SHE for 50 cycles at a scan rate of 100 mVs^{-1}, during which the atomic clusters are produced, that at the end of the 15th cycle itself, the deposit almost stops growing. This could be gauged by the saturation of current growth. However, in order to ensure uniform and maximum level of growth, we chose to employ 50 cycles for deposition. Under these conditions, surely a very adherent film of clusters is deposited over which additional growth occurs which is loosely bound to the electrode. Dedicated studies using scanning tunneling microscopy will be able to reveal details of these processes.

Differential Pulse Voltammetry: Fig.S1 shows the differential pulse voltammogram due to quantized double-layer charging of the gold clusters at the Pt microelectrode (10μm) in Bu_4NClO_4/CH_2Cl_2 [Pulse amplitude: 50 mV; pulse width: 50 ms; pulse period: 200 ms; scan rate: 20 mVs^{-1}]. Extremely low capacitive currents observed in the voltammograms show perfect nanoelectrode array behaviour [3]. We observed well defined peaks for the redox chemical character of the AuACs and the voltammograms have a large featureless central gap between the peaks (potential region from -1 V to 1.5 V vs quasi-Ag-reference. This gap is understood to be due to *molecule-like* electronic energy structure of the clusters arising from their sub-nanometer core dimensions with a rather substantial HOMO-LUMO gap [4].

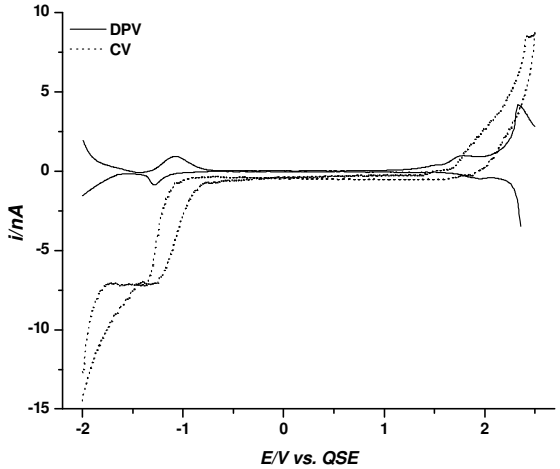

Fig.S1. DPV of AuACs (solid line) in 0.05 M Bu_4NClO_4/CH_2Cl_2 at Pt microelectrode. Pt coil counter electrode; Quasi-Ag-reference electrode (QSE) [Pulse amplitude: 50 mV; pulse width: 50 ms; pulse period: 200 ms; scan rate: 20 mVs^{-1}]. The corresponding CV at a scan rate of 20 mVs^{-1} is inserted (dotted line).

Experimental details for MALDI analysis: MALDI-TOF mass spectra were acquired using an Autoflex II TOF/TOF (Bruker Daltonics, Germany) spectrometer equipped with a standard UV nitrogen laser (337 nm). The matrix α-cyano-4-hydroxycinnamic acid (α-cyano, CHCA) was weighed accurately 5 mg and dissolved in 1 mL of 0.1 % Trifluroacetic acid:ACN (50:50 % v/v). 10 μL of the sample (clusters dissolved in CTAB/H_2O-solution form) was mixed with 10 μL of the matrix in a micro centrifuge tube (capacity: 500 μL). It was vortexed for 5 minutes at 2000 rpm to ensure the complete mixing of the content. The solution was found clear after vortexed. Then approximately 1 μL of premix sample was spotted onto clean MALDI plate and allowed to dry in air for about 15 minutes. Same procedure was followed for all the samples. Each sample was spotted in duplicate on MALDI plate. The plate was loaded in the MALDI – TOF setup. Ionization was achieved by irradiating the sample spots using UV

nitrogen laser at wavelength 337 nm and at an operating frequency of 25 Hz. The spectra were acquired in positive ionization and reflection mode with an acceleration voltage of 20.0 kV. In general, 200 laser shots were averaged for each spectrum. All spectra were processed using flex Analysis software version 2.4. An expanded version of Figure 2 in the main article is given at the end.

X-ray photoelectron spectroscopy: XPS analysis of the sample was done using the Multilab 2000 (Thermoscientific, UK) photoelectron spectrometer fitted with a twin anode x-ray source. The Au 4*f* core-level photoemission spectra were recorded using the MgK_{α} (1253.6.eV) source. Experimental data were curve fitted with a Gaussian and Lorentzian mix-product function after subtracting Shirley Background. Spin-orbit splitting and the doublet intensities were fixed as described in literature [5].

The Au4*f* core level photoelectron spectra of the AuACs deposited on Au foil electrode (Fig.S2) display two doublets for Au4$f_{7/2\text{-}5/2}$ at 84.46 & 88.16 eV and at 86.60 & 90.30 eV respectively. The first doublet of 4$f_{7/2}$ at 84.46 eV and 4$f_{5/2}$ at 88.16 eV can arise from the substrate Au foil. A shift from a value of 83.87 eV (Fig.2) observed for the same Au foil electrode before the deposition of AuACs could be due to the influence of the CTAB-supported AuACs deposited on it. The second doublet of 4$f_{7/2}$ at 86.60 eV and 4$f_{5/2}$ at 90.30 eV arises from CTAB-supported AuACs. A larger core-level B.E. shift of 2.2 eV observed for the deposited AuACs may be due to a combined influence of cluster size and the surfactant (Br containing CTAB) [6-8], leading to the stabilization of smaller core AuACs [9].

It is surprising to find a binding energy shift of this large magnitude, as the positive shift values reported for gold nanoclusters usually are around 0.6 eV. A shift in excess of this latter can arise due to the fact that Au(0) clusters experience a different chemical environment. More detailed structural investigations are needed to explain this large extent of binding energy shift.

1)

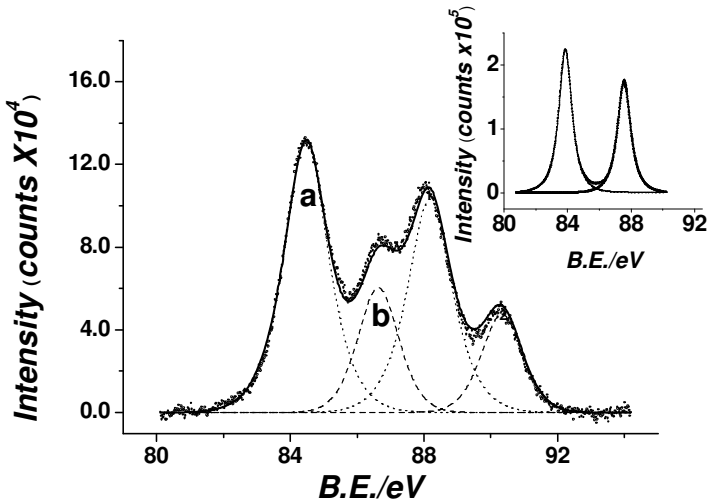

Figure S2: 1) X-Ray Photoelectron Spectra of AuACs on bulk gold substrate in Au 4f region. Black solid line is the fit to the observed data. Dotted line (a) and dashed line (b) corresponds to the AuACs and the Au substrate foil. Inset: Spectra of the Au foil before AuACs deposition;

2)

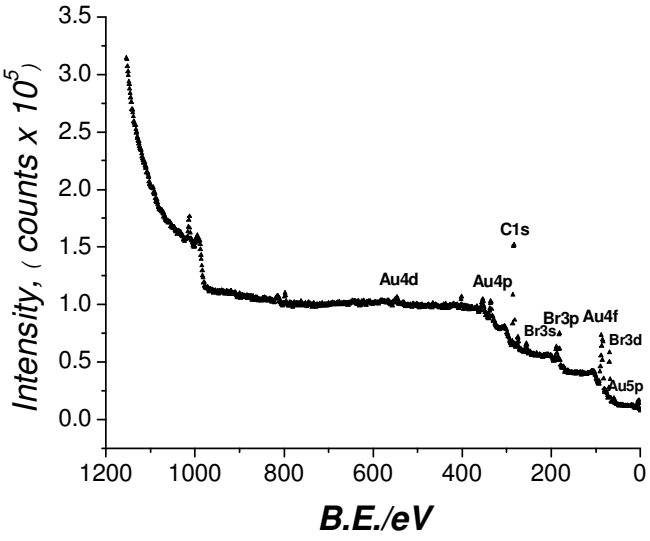

Figure S2: 2) Survey spectrum of AuACs on bulk gold substrate.

Transmission electron microscopy: Transmission electron microscopy was performed using Philips CM200 microscope working at 200 keV. The cluster solution was drop-cast on carbon-coated copper grid (400-mesh) for transmission electron microscopy. The electrochemically synthesized clusters were not accessible to imaging in the analytical transmission electron microscope (TEM) of resolution of a few nm when the as-prepared samples were examined on a carbon-coated copper grid was used. Difficulties in imaging sub-nanometer sized metal clusters have been detailed in refs. [10, 11]. However, with the cluster samples treated with acetone, spherical or rod-shaped particles were noticed [Fig.S3]. The corresponding selected area electron diffraction patterns are also given in the insets.

1) 2)

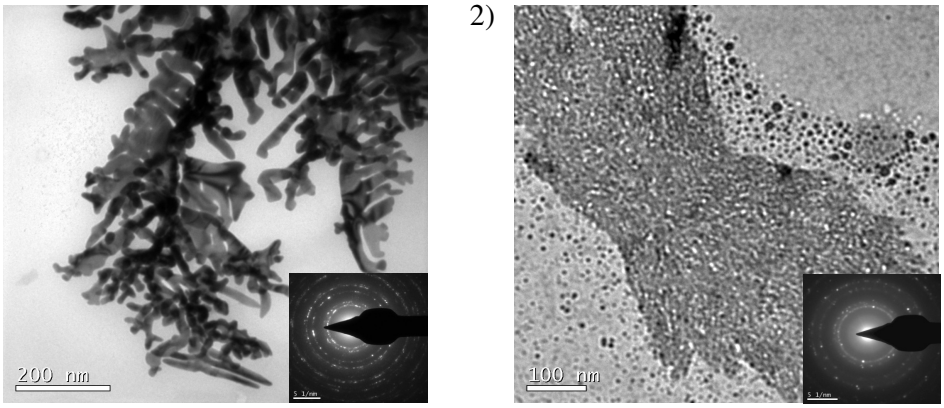

Fig.S3. Transmission electron micrograph of (1) rod-shaped and (2) spherical gold nanoparticles formed on addition of acetone to the atomic gold cluster solution.

Gold atomic clusters on GC: In order to ascertain if the gradual change-over of oxygen reduction mechanism on gold clusters ([CTAB] < cmc) from 4e-reduction to 2e-reduction is due to the cluster-aggregation or to the exposure of the underlying gold substrate, we collected the clusters on a second working electrode, viz., glassy carbon (GCE). During potential cycling of the gold disk in 0.1 mM CTAB, a GC electrode is also kept underneath the gold disk and connected to the same working electrode terminal in such a way that whatever the clusters are produced on the gold disk will eventually be deposited on the GC also. When this cluster-deposited GCE was employed for ORR in 0.5 M H_2SO_4, the initial scans showing voltammetric features corresponding to 4-electron transfer (O_2 to water) gradually changed to 2-electron transfer (O_2 to H_2O_2) (Fig.S4).

The transition from 4-electron to 2-electron reduction is also seen in this experiment with cluster-deposited glassy carbon surface. This observation clearly demonstrates that the transition is not due to bulk gold substrate, but to the conversion of clusters to nanoparticles caused by the instability of clusters in presence of sub-cmc concentration of CTAB. Further, to check if the material collected on glassy carbon is truly clusters, UV-visible absorption characteristics were analyzed. The spectra retained the molecule-like characteristics shown in Fig.1 (overlaid spectra) confirming the formation of clusters on gold substrate.

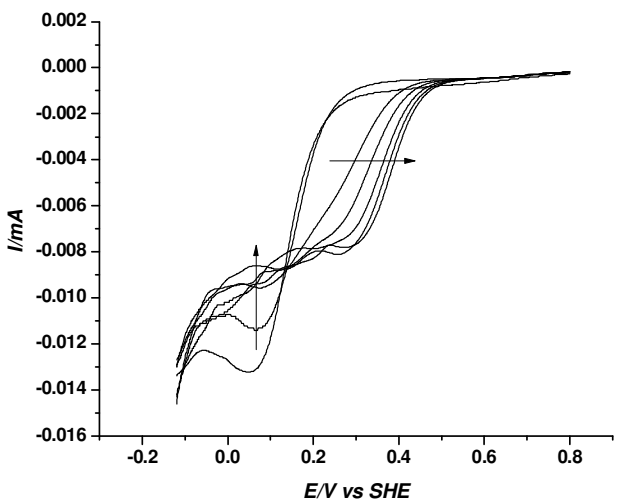

Fig.S4: Successive linear sweep voltammograms for ORR in oxygen-saturated 0.5 M H_2SO_4 solutions on AuACs electrodeposited on glassy carbon from 0.1 mM CTAB solutions. Scan rate: 5 mVs^{-1}. Arrows indicate direction of shift of current/potential (color markings are given only to identify individual LSV runs).

Hydrodynamic voltammetry (RDE & RRDE): Fig.S5 shows the rotating ring-disc (RRDE) voltammograms of ORR at the AuAC electrode in oxygen-saturated solutions of 0.5 M H_2SO_4 at various rotation rates (from 400 to 3600 rpm). Having established the basic features of ORR at gold cluster electrodes, it is opportune to evaluate its reaction kinetics using Koutecky-Levich analysis and the equation (1) is called Koutecky-Levich equation [12]:

$$\frac{1}{i} = \frac{1}{i_K} + \frac{1}{i_L} = \frac{1}{nFAkC_o} + \frac{1}{0.2nFAC_oD_o^{2/3}\nu^{-1/6}\omega^{1/2}} = \frac{1}{i_K} + \frac{1}{B\omega^{1/2}} \quad \ldots\ldots\ldots\ldots\ldots (1)$$

where i_K is the kinetic current, B is the Levich slope, n is the number of electrons involved in the ORR per oxygen molecule, C_o is the saturation concentration of oxygen in the electrolyte (1.26×10^{-3} M), D_o is the diffusion coefficient (1.93×10^{-5} cm^2 s^{-1}) and ν is the kinematic viscosity (1.009 cm^2 s^{-1}) and ω is the rotation rate in rpm. The kinetic parameters are arrived at using the K-L plots ($\omega^{-1/2}$ vs. i^{-1}). First-order kinetics of oxygen reduction is clear from the linearity and parallelism of the K-L plots. Considering the present data of RDE voltammograms, the number of electrons derived from K-L plots, the rate constant value and the comparison with the literature, there are strong evidences that the clusters produced in the present work are of the type, Au_n where n ≅ 3-11.The percentage of hydrogen peroxide, if generated, during the reduction of oxygen is calculated using the equation (2):

$$\%H_2O_2 = \frac{2I_R / N}{I_D + (I_R / N)} \times 100 \qquad \text{..... (2)}$$

where I_D and I_R are the disk and ring currents, respectively and N is the collection efficiency (0.21) of the Pt ring.

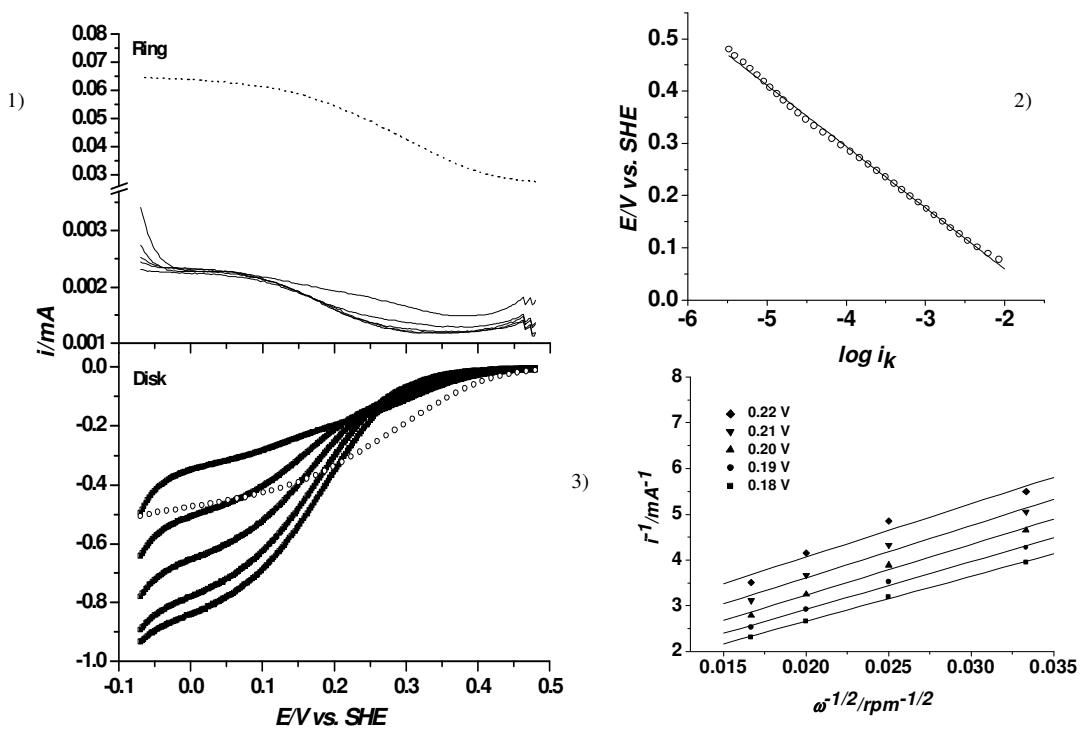

Fig.S5. (1) Rotating ring-disk measurements of oxygen reduction reaction on AuACs deposited on a gold disk (black) with a Pt ring at various rotation rates: 400, 900, 1600, 2500 and 3600 rpm. Dotted and hollow-circled line represents ring and disk response of ORR on bulk gold electrode, respectively, at 1600 rpm (Scan rate: 5 mVs^{-1}), (2) Tafel plot and (3) Koutecky-Levich Plot. Geometrical surface areas of the disk and ring are 0.283 cm^2 and 0.126 cm^2, respectively. (Platinum ring is used to sense the current due to reduction of hydrogen peroxide and in turn estimate the extent of formation of hydrogen peroxide)

Blank voltammetry of AuACs: Electro-oxidation of AuACs starts at potentials less anodic to that of bulk gold (both red and olive green lines), in consonance with the behaviour of small metal clusters. Apart from the differences in the voltammetric patterns of AuACs versus bulk gold electrode, the redox chemical character and the large featureless potential gap in the differential pulse voltammetry of AuAC-modified electrodes [Fig.S1] additionally vouch for the special voltammetric behaviour of small Au clusters.

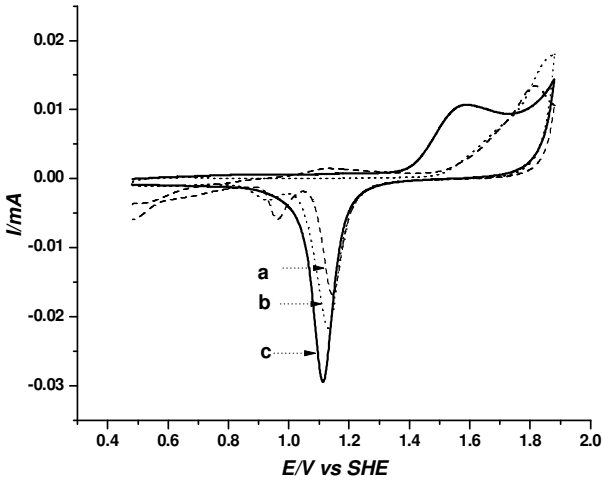

Fig.S6. Cyclic voltammograms of AuACs (a, dashed line = above cmc; b, dotted line = below cmc) and c, solid line = bulk gold (blue) in 0.5 M sulfuric acid at the scan rate of 100 mV.s^{-1}.

References

[1] K. Naoi, Y. Oura, M. Maeda, S. Nakamura, *J. Electrochem. Soc.* **1995**, *142*, 417.

[2] W. Cheng, S. Dong, and E. Wang, *Langmuir* **2003**, *19*, 9434.

[3] M. Fleischmann, S. Pons**,** D. Rolison and P. P. Schmidt, *Ultramicroelectrodes*, Datatech Systems, Morganton, NC, **1987**.

[4] Y. Y. Yang, S. W. Chen, *Nano Lett.* **2003**, *3*, 75.

[5] G. Selvarani, S. Vinod Selvaganesh, S. Krishnamurthy, G. V. M. Kiruthika, P. Sridhar, S. Pitchumani and A. K. Shukla, *J. Phys. Chem. C* **2009**, *113*, 7461.

[6] P. Zhang, T. K. Sham, *Phys. Rev. Lett.* **2003**, *90*, 245502.

[7] K. Takahiro, S. Oizumi, A. Terai, K. Kawatsura, B. Tsuchiya, S. Nagata, S. Yamamoto, H. Naramoto, K. Narumi, M. Sasase, *J. Appl. Phys.* **2006**, *100*, 084325.

[8] H. G. Boyen, A. Ethirajan, G. Kastle, F. Weigl, P. Ziemann, G. Schmid, M. G. Garnier, M. Buttner, P. Oelhafen, *Phys. Rev. Lett* **2005**, *94*, 016804.

[9] H. G. Boyen, G. Kastle, F. Weigl, P. Ziemann, G. Schmid, M. G.Garnier, P. Oelhafen, *Phys. Rev. Lett.* **2001**, *87*, 276401.

[10] L. D.Meard, H. Gao, R. D.Xu, A. S.Twesten, Y. Harper, G. Song, A. D.Wang, J. C. Douglas, A. I. Yang, R. G.Frenkel, R. Nuzzo, R. W. Murray, *J. Phys. Chem. B* **2006**, *110*, 12874.

[11] S. Ijima, T. Ichihashi, *Phys. Rev. Lett.* **1986**, *56*, 616.

[12] A. J. Bard, L .R. Faulkner, *Electrochemical Methods: Fundamentals and Applications*, John Wiley & Sons, New York, **2001**, Second edition, Chapter 9, pp. 331-367.

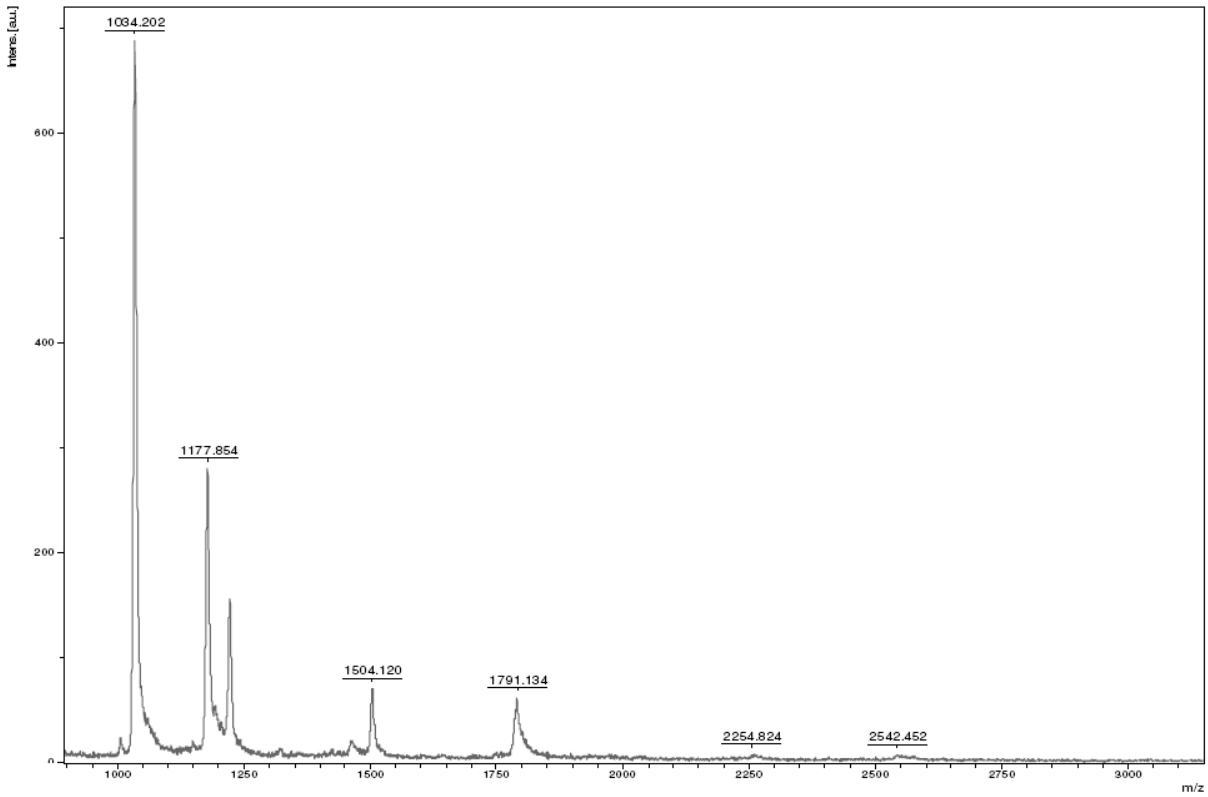

Mass Spectrum-Expanded version of Figure 2 in main article

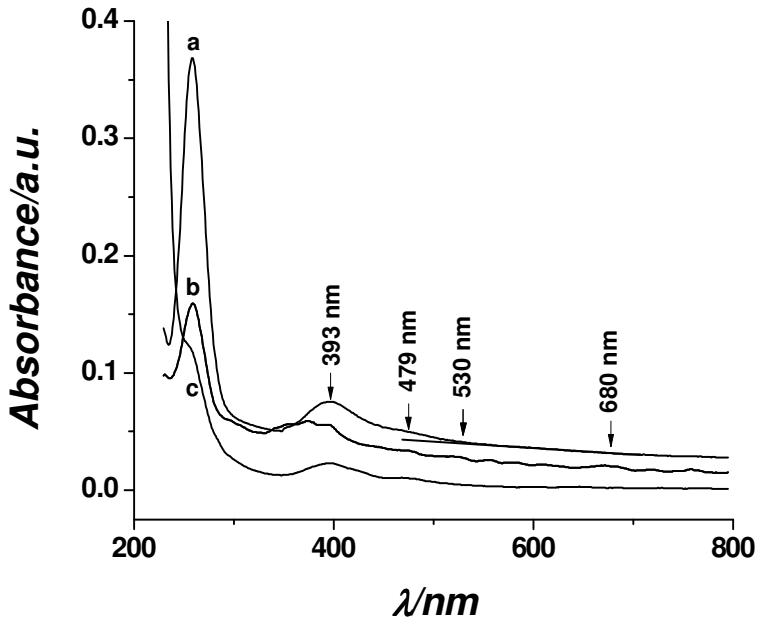

Expanded version of Figure 1 in the main article